Studies on stability in three-layer Hele-Shaw flows

Prabir Daripa[a)]
Department of Mathematics, Texas A&M University, College Station, Texas 77843, USA

(Received 21 September 2007; accepted 29 September 2008; published online 13 November 2008)

We consider a setup in a Hele-Shaw cell where a fluid of constant viscosity μ_l occupying a near-half-plane pushes a fluid of constant viscosity $\mu > \mu_l$ occupying a layer of length L which in turn pushes another fluid of constant viscosity $\mu_r > \mu$ occupying the right half-plane. The fluid upstream has a velocity U. Careful analysis of the dispersion relation arising from linear stability of the three-layer Hele-Shaw flow problem leads to the following specific analytical results all of which are strikingly independent of the length (L) of the middle layer: (i) a necessary and sufficient condition for modal instability; (ii) a critical viscosity of the middle layer that gives the shortest bandwidth of unstable waves; and (iii) a strict upper bound on the growth rate of instabilities, meaning that this upper bound is never reached and hence this upper bound can be improved upon. Results based on exact growth rates are presented which provides some insight into the instability transfer mechanism between interfaces as the parameters of the problem are varied. Numerical evidence that supports the effectiveness of the upper bound is also presented. © *2008 American Institute of Physics*. [DOI: 10.1063/1.3021476]

I. INTRODUCTION

Studies in three-layer Hele-Shaw flows are of interest to several industrial processes, enhanced oil recovery (EOR) process is one of them, and also to our basic understanding of hydrodynamic stability in multiphase flows. Hele-Shaw models are simplifications of saturation models [models involving Buckley–Leverett (see Ref. 1) equations] that are closer to actual physics in porous media flows, but these simpler models allow studies of certain aspects of physics in isolation that are prevalent in porous media flows. For example, saturation shocks (discontinuities in saturation) in saturation models have across them different effective viscosities and propagate with speed faster than the fluid speed behind these shocks. On the other hand, discontinuities in Hele-Shaw models based on Darcy's law [see Eq. (1) and the text following Eq. (1)] are of contact types, meaning that these are material interfaces which travel in its normal direction at the same speed as the speed of fluids on either side of these interfaces, though the fluids themselves may have different viscosities. Therefore, Hele-Shaw models allow one to distinguish the viscosity effect from the influence of nonlinear waves which would otherwise be present in saturation models. It is also a step toward an ability to better understand any flow complexity arising solely due to the presence of saturation waves in saturation models. This has a bearing in the development of effective and economical strategies for controlling interfacial instabilities that play a critical role in many industrial processes including EOR in porous media.

It is well known that in a two-layer Hele-Shaw flow where a viscous fluid (with viscosity μ_r) such as oil is displaced by another less viscous immiscible fluid (with viscosity $\mu_l < \mu_r$) such as water, the material interface separating these two immiscible fluids of different viscosities suffers from Saffman–Taylor (ST) instability[2] with surface tension playing an important role in mitigating growth rates of the disturbances. For a review on this instability, see Refs. 3 and 4. An analogous instability in porous media has been studied by Chouke *et al.*[5] A straightforward extrapolation of this phenomenon to a three-layer case in a Hele-Shaw cell suggests that addition of a middle layer in an otherwise two-layer Hele-Shaw flow can reduce the growth rates of instabilities on the leading interface significantly provided $\mu_l < \mu < \mu_r$ with μ being the viscosity of the fluid in the middle layer. The origin of this idea dates back to the early 1960s from the basic work on ST instability and has since attracted much attention, with most of the literature reviewed and systemized first by Shah and Schechter[6] and then by several other authors (see Refs. 7–9) in recent years.

Polymer augmented chemical flooding has been very popular (e.g., see Refs. 7, 9, and 10) because the role of the polymer is to increase the viscosity, reducing the mobility ratio and hence allowing a greater volumetric swept efficiency. In fact, one of the chemical EOR processes involves injection of chemical agents such as polymer in water to increase the viscosity of the displacing fluid so that the ST instability of the interface is somewhat mitigated. Henceforth, such displacing fluid containing polymer will be called polysolution. Since polymer is expensive, injection of polysolution is usually followed by injection of pure water to keep the cost low so that the recovery process is economically viable. Thus, this chemical EOR process involves a three-layer flow. To take advantage of and better understand this three-layer oil recovery process involving polymer flood, there have been some numerical studies of Hele-Shaw models[11] as well as saturation models[12] for this chemical EOR process in porous media.

In Ref. 12 the above mentioned chemical EOR process in porous media is modeled by a coupled system of elliptic and hyperbolic equations which is then numerically solved

a)Electronic mail: prabir.daripa@math.tamu.edu.

using a front-tracking method. The numerical study there exclusively focused on the effect of middle-layer viscosity on (i) sweeping efficiency and improvement of oil recovery in quarter-five-spot geometry and (ii) interfacial interactions in a Hele-Shaw cell geometry. In spite of such studies and available software that solves this specific EOR process by polymer flooding, industrial use of this chemical EOR process is less than that of other EOR processes because of several factors some of which are (i) the cost involved in using polymer agent for increasing viscosity, (ii) difficulty in identifying most effective type of polymer solution due to complicated rheological properties, (iii) dynamic absorption of polymers and dynamic changes in the structures of polymers during flow process which complicates the modeling process, (iv) difficulty in obtaining accurate quantitative estimates as not all physical mechanisms involved are well understood, and (v) lack of understanding of hydrodynamic stability issues associated with three-layer flows.

Our interest here is in advancing our understanding of hydrodynamic stability issues associated with three-layer flows, some of which are listed below.

- Bandwidth of unstable waves: Whereas it is true that the existence of unstable band determines instability, it is the width of the band and the wave structures in it that should help in devising instability control strategy. For example, if the band is too wide then designing a process that can inhibit growth of waves in this band will likely be different from what it would be if the band were too narrow. Also, the wavelengths of the unstable waves matter in dictating the control strategies. For example, if the disturbances in this unstable band can be carefully avoided or considerably reduced, then onset of undesirable fingering phenomenon in the context of chemical EOR can be significantly delayed which can be helpful to enhance oil recovery. In fact, such measures are commonplace in a related subject: transition to turbulence. To cite an example, in-plane Poiseuille flow experiments show that transition to turbulence occurs at Reynolds number of the order of 1000 (see Ref. 13), even though with control of disturbances the transition to turbulence can be delayed to Reynolds number of the order of 10^5 (see Ref. 14). Therefore, from an instability control viewpoint in chemical EOR it is important to know the dependence of the unstable band (its width and the waves it contains) on the parameters of the problem, in particular, the viscosities of three fluids in three layers, the interfacial surface tensions, and the length of the middle layer so that one or more of these can be controlled and exploited to reduce the growth rates of leading interfacial instabilities which have direct bearing on EOR.

  As such the unstable band plays a much more fundamental role in its ability to qualitatively predict the complexity of evolution of interfaces past the linear stage. For example, if the unstable band is too narrow, then only a few modes initially participate in describing the evolution of initial disturbance whereas if the band is too broad, then more waves will do so, creating more waves through nonlinear interaction within a short time. Thus it is very likely that interfacial geometry, immediately past the linear stage, will be more complex for broad unstable band than for a narrow unstable band. The exact location of this unstable band in the wave-number space has a role to play on the nature of complexity of interfacial geometry. For example, if the band is too broad with too many unstable short waves, then the interface is likely to develop fine-scale structures very quickly, whereas if the unstable waves are too long, then the interface is likely to have large scale features. In any case, knowledge of unstable band is important which has the potential to allow design of effective instability control strategies and to predict in a qualitative sense the extent of complexity of interfacial evolution past the linear stage. In particular, note the following.
- Upper bound of the growth rate: It is essentially the growth rate of the most dangerous wave if the upper bound is a good estimate of the growth rate. Controlling this, i.e., somehow reducing this growth rate by some strategy, certainly allows control over interfacial instability. However, design of such strategies first requires determining the dependence of this maximal growth rate on other parameters of the problem. In this sense, the upper bound of the growth rate is an important issue that needs careful estimation.
- Optimal (shortest) size of the middle layer: Intuition as well as numerical studies (see Ref. 12) suggest that incremental gain in stabilization of the leading interface due to incremental increase (by some fixed amount) in the size of the middle layer gradually decreases until such time that virtually no gain is obtained by further increasing the size of the middle layer. Thus, there is an optimal finite size of the middle layer which will certainly depend on the other parameters of the problem. Knowledge of this optimal size of the middle layer, even if it is based on linear theory, can be very useful for instability control purposes as well as in minimizing the cost of those chemical EOR processes where the higher viscosity of the middle layer is usually obtained by using polymer in water.

Since one of the reasons behind using polymer in these three-layer chemical EOR processes is to stabilize the leading interface, it is natural to try to first understand these stability issues associated with three-layer flows. Then, it may be more beneficial for the development of even more effective chemical EOR process than currently available. In this paper, we present a simplified exact linearized stability analysis of Hele-Shaw model equations and some numerical calculations that provide some insight into these issues.

At this point, it is important to emphasize that results based on linear theory can rarely predict ultimate nonlinear evolution of fronts at late times. Rather, these results based on linear theory allow hopes for designing effective strategies to mitigate early-time growth of disturbances whose evolution through subsequent nonlinear interactions can

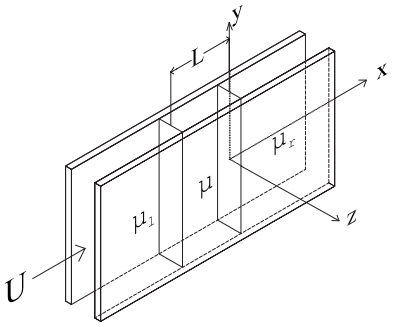

FIG. 1. Three-layer fluid flow in a Hele-Shaw cell.

mitigate the extent of fingering phenomenon at late times. For example, there is enough numerical evidence (see Ref. 12) that if the maximum rate of instability is reduced by increasing viscosity behind the leading front, then ST dynamics does ultimately describe the front in the sense that complexity of the interface and fingering effect are less severe. In this sense, results based on linear theory are useful.

The three-layer setup (see Fig. 1) that is of interest for these purposes has a fluid of constant viscosity μ_l which pushes a fluid of constant viscosity $\mu > \mu_l$ which in turn pushes another fluid of constant viscosity $\mu_r > \mu$. Two extreme layers are of infinite extent and the middle layer is of length L. The fluid upstream has a velocity U. The surface tension at the left interface is S and that at the right interface is T. The left interface across which the fluid viscosities are μ_l and μ will be called trailing interface henceforth. Similarly, the right interface separating the most viscous fluid with viscosity μ_r and the middle layer with viscosity μ will be called leading interface henceforth. This rectilinear Hele-Shaw flow with uniform velocity U and with two planar interfaces is an exact solution of the underlying equations of motion. Linearization of the governing equations and boundary conditions about this basic flow leads to a nontrivial (due to boundary conditions) eigenvalue problem for disturbances which retains the interaction of interfacial disturbances. We analytically and numerically analyze this eigenvalue problem in this paper. The exact dispersion relation provides a constructive method for evaluating the growth rates of disturbances which we numerically analyze to gain insight into the role of various parameters in reducing instability of the leading interface. As we will see, the dispersion relation is quadratic in the growth rate σ for each wave disturbance characterized by wave number k. Thus for each k, we will have two roots in general which we denote below as σ_+ and σ_-. In this paper, we refer each pair (k,σ) as a mode.[15] As a result, for each wave k there are two independent modes $[k,\sigma_+(k)]$ and $[k,\sigma_-(k)]$ that differ in this paper (as we will see later) by the interface they associate with as we have two interfaces. Below, we stick with this definition for a mode.

Right at the outset, we should mention the results obtained and the issues addressed in this paper which are the following.

(1) Using normal mode analysis, it is shown here that a necessary and sufficient condition for instability of a mode with wave number k is

$$k^2 \leq \min([\mu - \mu_l]U/S, [\mu_r - \mu]U/T).$$

Thus, note that this bandwidth of unstable waves is independent of the length L of the middle layer. We also note that a necessary (but not sufficient) condition for a mode to be unstable is

$$k^2 \leq \max([\mu - \mu_l]U/S, [\mu_r - \mu]U/T).$$

Indeed, if $\min(k_1,k_2) < k < \max(k_1,k_2)$, one mode is stable.

(2) We show the existence of a critical viscosity $\mu_{\rm cr}$,

$$\mu_{\rm cr} = \mu_l + \frac{S}{S+T}(\mu_r - \mu_l) = \mu_r - \frac{T}{S+T}(\mu_r - \mu_l),$$

of the middle layer that gives the shortest bandwidth $k_{\rm cr}$, given by

$$k_{\rm cr} = \sqrt{\frac{U}{S+T}(\mu_r - \mu_l)},$$

of unstable modes, meaning that every mode with $k > k_{\rm cr}$ has corresponding $\sigma_+ < 0$ and $\sigma_- < 0$. Both of these are also independent of L. We discuss later the significance of this critical viscosity.

(3) Eigenvalues (growth rates) are computed in parameter space which are graphically displayed to provide an understanding of interfacial instability transfer mechanism based on the principle of dominant eigenvalue.

(4) Analysis shows that gain in stabilization of the leading interface drops exponentially with increasing L and therefore most of the gain in stabilization is to be expected for small values of L as confirmed by results from numerical experiments. Numerically, we show existence of an optimal choice of the length L of the middle layer beyond which hardly any gain in stabilization can be obtained for any given set of parameter values μ, μ_r, μ_l, S, and T.

(5) Using a weak formulation of the underlying equation for disturbance, we derive an upper bound σ_u given by

$$\sigma < \sigma_u = \max\left\{\frac{2T}{\mu_r}\left(\frac{U(\mu_r - \mu)}{3T}\right)^{3/2}, \frac{2S}{\mu_l}\left(\frac{U(\mu - \mu_l)}{3S}\right)^{3/2}\right\},$$

on the growth rate which is independent of the length L of the middle layer. Since adding an intermediate layer $(\mu_l < \mu < \mu_r)$ in an otherwise two-layer flow should reduce maximal pure ST growth rate σ_{sm} based on viscosities μ_l and μ_r and a surface tension value equal to minimum of S and T, this σ_{sm} is also an upper bound. Therefore, an improved upper bound is minimum of these two upper bounds: σ_u and σ_{sm}. Numerical results are presented which compare these two upper bounds.

Much of the above studies on multilayer flows has provided a better understanding, though qualitative in nature, of the effect of interfacial viscosity jumps but less so of the effect of interfacial surface tensions even though interfacial surface tensions play an important role. An interesting effect of the surface tension in three-layer flows that will be exemplified later in this paper can be explained easily if we neglect, for the sake of explanation, interfacial interactions and

allow two-layer ST results to hold at each of the interfaces. Now, we assume that we continuously decrease the length of the middle layer which has no effect within our crude approximation until the length of this middle layer becomes infinitesimally small when this thin layer effectively acts as one merged interface with an increase in effective viscosity jump across it and also an increase in effective surface tension which now equals the sum of the two individual interfacial surface tensions (we emphasize that interfaces are distinct and infinitesimally close with middle-layer fluid still present). An increase in viscosity jump will try to increase the growth rate whereas an increase in effective surface tension will try to reduce the growth rate. These competing forces ultimately can either decrease or increase the growth rate of the leading interface depending on the specific values of various viscosities and surface tension parameters. It is easy to see using the above arguments in reverse (i.e., thickness of the layer increasing from almost zero thickness to finite thickness), that adding a middle layer having a viscosity μ with $\mu_l < \mu < \mu_r$ (see Fig. 1) need not necessarily stabilize the flow, which is contrary to our conventional belief in this context, unless the viscosity jump across the trailing interface exceeds a surface tension dependent threshold. Even though these remarks are based on gross simplifications as mentioned above where the interfacial growth rates are completely decoupled, it will be shown here through exact calculation within linear theory which retains the coupling between the interfacial growth rates that the above remarks based on simplified arguments hold true.

Finally, let me stress right at the outset that the goal of this paper, most broadly speaking, is to point out two major features of this problem through precise and simple calculations that are physically interesting as well: (i) there are certain important stability characteristics that are independent of the length of the middle layer which is counterintuitive. Fine details on this are itemized above and more on this are embedded in the text of the paper. (ii) There are some other characteristics (such as maximal growth rate) that depend on the length of the middle layer. These and some other results derived in this paper through what may appear to be a routine calculation of a simple ordinary differential equation with nonstandard boundary conditions are indeed new, interesting, and physically appealing. We also would like to mention that some aspects of this paper laid out in Sec. II are very close to previous work in the literature, especially the work of Gorell and Homsy[11] and Daripa and Pasa.[16]

This paper is laid out as follows. In Sec. II, we present relevant equations for three-layer Hele-Shaw flows, each layer containing a fluid of constant viscosity. In Sec. III, we obtain a band of unstable waves and a necessary and sufficient condition for a wave to be unstable. We also derive a quadratic equation in the growth rate whose roots give the dispersion relation. Upper bounds on the growth rate of disturbances are derived in Sec. IV. Finally, we conclude in Sec. V.

II. THREE-LAYER HELE-SHAW FLOWS

The model we consider within Hele-Shaw approximation consists of three regions as shown in Fig. 1. Because of averaging in the thin gap approximation (see below), the flow is two dimensional in the x-y plane. Therefore, the domain of interest is $\Omega := (x,y) = \mathbb{R}^2$ (with a periodic extension of the setup in the y direction). Thus this two-dimensional flow consists of a near-half-plane of water (leftmost region) stretching to $x \to -\infty$, similar to oil (rightmost region) stretching to $x \to \infty$, with a middle layer of polysolution in between. The polysolution in the middle layer of length L has a constant viscosity μ with $\mu_l < \mu < \mu_r$, where μ_l and μ_r are constant viscosities of the water and the oil phases, respectively.

The fluid upstream (i.e., as $x \to -\infty$) has a velocity $\mathbf{u} = (U,0)$. The relevant equations for this flow are then given by

$$\nabla \cdot \mathbf{u} = 0, \tag{1a}$$

$$\nabla p = -\mu \mathbf{u}, \tag{1b}$$

$$\frac{D\mu}{Dt} = 0, \tag{1c}$$

where p is the pressure, $\nabla = (\partial/\partial x, \partial/\partial y)$, D/Dt is the material derivative, $\mu = \mu_l$ for the leftmost layer, and $\mu = \mu_r$ for the rightmost layer. Equation (1a) is the continuity equation for incompressible flow, Eq. (1b) is the Darcy law, and Eq. (1c) is the advection equation for viscosity.[11,17] There is a rich history in fluid mechanics (see review articles of Saffman[3] and Homsy[4]) to using Darcy's law [Eq. (1b)] for modeling Hele-Shaw flow within thin-gap approximation. In fact, Eq. (1b) is obtained from averaging parabolic velocity profile in between the plates. Thus $\mathbf{u}$ in the system of equations above is a velocity to be understood in an average sense, and as a result our model does not account for the effect of structure of displacement in the gap between the plates. There is a reasonably complete mathematical and engineering literature on Darcy's law in thin regions (see Ref. 18 for averaging of creeping flow and Ref. 19 for averaging of the Navier–Stokes system). The derivation of Darcy's law for a periodic porous rigid medium using the homogenization theory is outlined in Ref. 20 (see Chap. 7, p. 129). See also pages 161–163 of Ref. 21. Regarding the effect of the structure of displacement in the gap between the plates on the Hele-Shaw model, see Ref. 22 for two-phase displacement and Ref. 23 for three-phase displacement. There it has been shown that in a certain limit this Hele-Shaw problem is best modeled by a hyperbolic equation with nonconvex flux function similar to the saturation model for porous media flows. Lastly, we should mention that there are other people who have tried to model the EOR process with miscible equations.[24] Toward this end, we should cite Ref. 25.

The above system admits a simple basic solution, namely, the whole fluid setup moves with speed U in the x direction and two interfaces, namely, the one separating the left layer from the middle layer and the other separating the right layer from the middle layer, are planar, i.e., parallel to the y axis. The pressure corresponding to this basic solution

is obtained by integrating Eq. (1b). In a frame moving with velocity $(U,0)$, the above system is stationary along with two planar interfaces separating these three fluid layers. Here and below, with slight abuse of notation, the same variable x is used in the moving reference frame.

In linearized stability analysis by normal modes, disturbances in the moving reference frame are written in the form $(\tilde{u},\tilde{p})=[f(x),\psi(x)]e^{(iky+\sigma t)}$ and then inserted into the linearized disturbance equations obtained from Eq. (1) and also into the linearized dynamic and kinematic interfacial conditions (see Ref. 16). After some algebraic manipulation of the resulting equations in $f(x)$ and $\psi(x)$, we obtain the following problem for the eigenfunction f:

$$f_{xx}-k^2f=0, \quad x\in(-L,0), \tag{2a}$$

$$f_x(0)=(\lambda p+q)f(0), \quad f_x(-L)=(\lambda r+s)f(-L), \tag{2b}$$

where $\lambda=1/\sigma$, and p, q, r, and s are defined by

$$p=\{(\mu_r-\mu)Uk^2-Tk^4\}/\mu, \quad q=-\mu_r k/\mu\le 0,$$
$$r=\{(\mu_l-\mu)Uk^2+Sk^4\}/\mu, \quad s=\mu_l k/\mu\ge 0. \tag{3}$$

Note that

$$p\ge 0 \quad \text{for } k^2\le k_2^2=(\mu_r-\mu)U/T \quad \text{and}$$
$$r\le 0 \quad \text{for } k^2\le k_1^2=(\mu-\mu_l)U/S. \tag{4}$$

III. DISPERSION RELATION AND ITS ANALYSIS

The general solution $f(x)=A\exp(-kx)+B\exp(kx)$ (where A and B are constants) of Eq. (2a) for the domain $-L\le x\le L$ is substituted in the boundary conditions in Eq. (2b), which leads to a matrix equation $MX=0$ for the unknown constant vector $X=(A,B)$. The matrix M is given by

$$M=\begin{pmatrix} e^{kL}(\sigma(\mu+\mu_l)+\tau) & e^{-kL}(\sigma(-\mu+\mu_l)+\tau) \\ \sigma(\mu-\mu_r)+\xi & \sigma(-\mu-\mu_r)+\xi \end{pmatrix}, \tag{5}$$

where

$$\tau=\frac{\mu r}{k}=Sk(k^2-k_1^2) \quad \text{and} \quad \xi=\frac{\mu p}{k}=Tk(k_2^2-k^2). \tag{6}$$

The solvability condition $\det(M)=0$ for a nontrivial solution then leads to the dispersion relation

$$a\sigma^2+b\sigma+c=0, \tag{7}$$

where the coefficients a, b, and c are given by

$$a=-e^{kL}(\mu+\mu_l)(\mu+\mu_r)+e^{-kL}(\mu-\mu_l)(\mu-\mu_r)<0, \tag{8a}$$

$$c=\tau\xi(e^{kL}-e^{-kL}), \tag{8b}$$

$$b=[e^{kL}(\mu+\mu_l)+e^{-kL}(\mu-\mu_l)]\xi - [e^{kL}(\mu+\mu_r)+e^{-kL}(\mu-\mu_r)]\tau. \tag{9}$$

Below, we use for the roots of Eq. (7) the following notations:

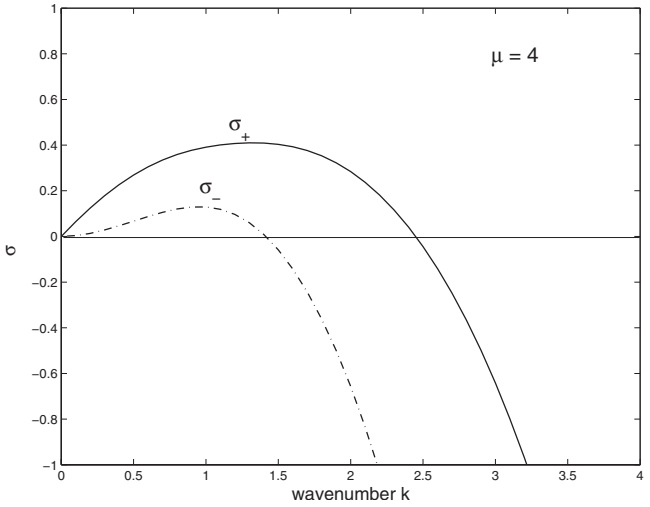

FIG. 2. Dispersion relation: growth rates σ_- and σ_+ vs wave number k when $\mu=4<\mu_{cr}=6$ [equivalently $k_2(=\sqrt{6})>k_1(=\sqrt{2})$] for parameter values $\mu_l=2$, $\mu=4$, $\mu_r=10$, $T=S=U=1$, $L=1$. Here $\sigma_-(k_1)=0$ and $\sigma_+(k_2)=0$ where k_1 and k_2 are defined as $k_1=\sqrt{(\mu-\mu_l)U/S}=\sqrt{2}$ and $k_2=\sqrt{(\mu_r-\mu)U/T}=\sqrt{6}$.

$$\sigma_-=(-b+\sqrt{b^2-4ac})/2a \quad \text{and} \quad \sigma_+=(-b-\sqrt{b^2-4ac})/2a. \tag{10}$$

Growth rates σ_- and σ_+, as will be shown later [see text after Eq. (16)], are real.

The dispersion relations above are somewhat cumbersome in terms of wave number k due to the nature of dependencies of a, b, and c on k. A plot of these dispersion relations for some choices of parameter values is given in Fig. 2. For all wave numbers $k>0$, $\sigma_+>\sigma_-$ in Fig. 2. However, for some choices of parameter values these dispersion curves can contact each other at a wave number but cannot cross each other because $\sigma_+-\sigma_-=-\sqrt{b^2-4ac}/a$ cannot be negative [see Eqs. (8a) and (10)] for any value of k. The fact that these dispersion curves can contact each other for some values of parameters is discussed in Secs. III A and III B.

A. Existence of a neutral wave

A wave having $\sigma_+=\sigma_-=0$ is referred to here as a neutral wave. It is easy to see from Eqs. (6)–(9) that $\sigma_-(k)=\sigma_+(k)=0$ if and only if $k=0$ or $k=k_1=k_2$. This establishes the existence of a nontrivial neutral wave $k=k_1=k_2$. This criterion for the existence of a nontrivial neutral wave, upon using the definitions of k_1 and k_2 from Eq. (4), translates into

$$\frac{\mu-\mu_l}{\mu_r-\mu}=\frac{S}{T}, \tag{11}$$

which gives viscosity μ of the middle-layer fluid in terms of the extreme layer fluid viscosities and interfacial surface tensions. Henceforth, we call this *critical* viscosity and denote by μ_{cr}. Similarly, we call the wave number $k=k_1=k_2$ of the neutral mode critical wave number and denote it by k_{cr}. Thus

$$\mu_{cr}=\mu_l+\frac{S}{S+T}(\mu_r-\mu_l)=\mu_r-\frac{T}{S+T}(\mu_r-\mu_l) \tag{12}$$

and

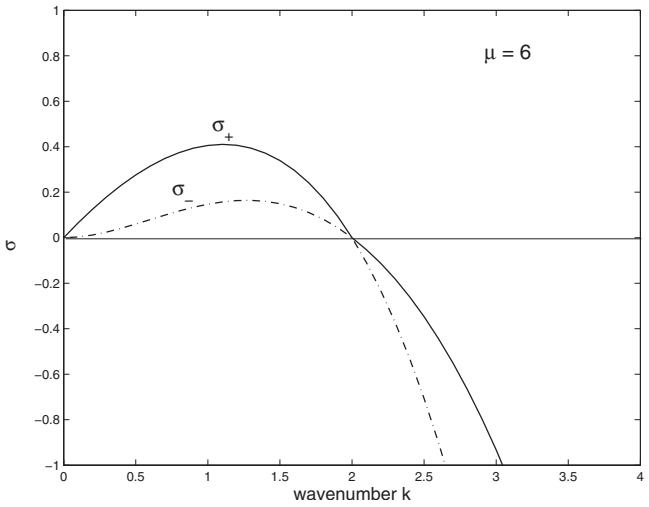

FIG. 3. Dispersion relation: growth rates σ_- and σ_- vs wave number k when $k_1(=2)=k_2(=2)$ for parameter values $\mu_l=2$, $\mu=6$, $\mu_r=10$, $T=S=U=1$, $L=1$.

$$k_{\rm cr}=\sqrt{\frac{U}{S+T}(\mu_r-\mu_l)}. \tag{13}$$

Thus, $\mu=\mu_{\rm cr}$ is an alternate form of the criterion for the existence of a nontrivial neutral wave. This neutral wave has wave number $k=k_{\rm cr}$. Plots of the dispersion relations for parameter values satisfying criterion (12) are shown in Fig. 3. This figure shows that $\sigma_-=\sigma_+=0$ at $k=k_{\rm cr}$ given by Eq. (13). It is important to emphasize that two dispersion curves in this plot merely contact (and not cross) each other at $\sigma_-=\sigma_+=0$. Below, the range of wave numbers for which at least one of the two eigenvalues is positive is called the width of the unstable band. Thus, in Fig. 3 the width of the unstable band is $k_{\rm cr}$. It is worth noting that length L of the middle layer has no effect either on the above criterion (12) or on the wave number (13) of the neutral wave.

B. Existence of a nonneutral wave with $\sigma_-=\sigma_+$

In Sec. III A, we saw that two dispersion curves given by Eq. (10) contact each other at $(k,\sigma)=(k_{\rm cr},0)$ when $\mu=\mu_{\rm cr}$. A natural question in this context is whether there are other choices of parameter values for which these two dispersion curves contact each other for a disturbance and if they do, what are the wave number $k_*>0$ and corresponding growth rate σ_* $(=\sigma_-=\sigma_+\neq 0)$ of the disturbance.

If $\min(k_1,k_2)<k<\max(k_1,k_2)$, then it follows from Eq. (6) that $\tau\xi>0$ and hence $c>0$ from Eq. (8b). Therefore the radical b^2-4ac of the quadratic Eq. (7) cannot be zero and two roots σ_- and σ_+ cannot be equal regardless of the values of L and other parameters. Then we conclude that if these two dispersion curves contact each other at $(k_*,\sigma_*\neq 0)$, then either $k_*<\min(k_1,k_2)$ or $k_*>\max(k_1,k_2)$. As a result, τ and ξ [see Eq. (6)] have opposite signs and hence $b\neq 0$ and $c<0$ [see Eqs. (8b) and (9)] at $k=k_*$. Therefore, the radical b^2-4ac can be zero at an admissible value of $k=k_*$ for some, not every, choice of parameter values in which case $\sigma_-(k_*)=\sigma_+(k_*)=-b/(2a)$. If $0<k_*<\min(k_1,k_2)$, then $\sigma_-(k_*)=\sigma_+(k_*)>0$ which follows from the fact that $b>0$ [see Eqs. (6) and (9)]. Similarly, if $k_*>\max(k_1,k_2)$, then $\sigma_-(k_*)=\sigma_+(k_*)<0$. For some parameter values, it is conceivable that the $\sigma_-=\sigma_+$ condition may lead to the condition $k^2\leq 0$ which would simply mean that these two dispersion curves do not contact with each other at any value of k. For the parameter values for which the study is conducted and discussed later, there is no such k_* (see Sec. III E).

C. Width of the unstable band

The range of wave numbers for which flows are unstable is important for the purpose of control and understanding of flows as we have discussed before in Sec. I. Figure 2 shows that each of the two eigenvalues is zero at a wave number distinct from the other one. A simple investigation of the dispersion relation shows that if $k=k_1$ or $k=k_2$ then $c=0$, and as a result $\sigma_-(k_1)=\sigma_+(k_2)=0$ if $k_2>k_1$ and $\sigma_+(k_1)=\sigma_-(k_2)=0$ if $k_2<k_1$. If $k^2<\min(k_1^2,k_2^2)$, then $b>0$, $c<0$ from Eqs. (6), (8b), and (9). Therefore $\sigma_-\sigma_+=c/a>0$ and $\sigma_-+\sigma_+=-b/a>0$, and hence both σ_- and σ_+ are positive for all waves with $k<\min(k_1,k_2)$. Similarly, it is easy to verify that one of these two roots will be positive and the other one negative for all waves in the band $\min(k_1,k_2)<k<\max(k_1,k_2)$. Putting together these facts [and keeping in mind the notation k_1 and k_2 introduced in Eq. (4)], we conclude that at least one of these two eigenvalues is positive if wave number k satisfies

$$k\leq \max(k_1,k_2)=\max\left\{\sqrt{\frac{(\mu-\mu_l)U}{S}},\sqrt{\frac{(\mu_r-\mu)U}{T}}\right\}. \tag{14}$$

Thus, this is a necessary (but not sufficient) condition for instability of a mode with wave number k. In Fig. 3, k_1 and k_2 are nontrivial zeros of the two eigenvalues. The right hand side of the above equality is the width of the unstable waves in wave number space. Note that this bandwidth of unstable waves is also independent of the length L of the middle layer. It also follows from our discussion in the previous paragraph that a mode is unstable if the corresponding wave number k satisfies

$$k\leq \min(k_1,k_2)=\min\left\{\sqrt{\frac{(\mu-\mu_l)U}{S}},\sqrt{\frac{(\mu_r-\mu)U}{T}}\right\}. \tag{15}$$

This is a necessary and sufficient condition for instability of a mode with wave number k.

Two eigenvalues σ_- and σ_+ for each wave number k essentially arise because of two interfaces. For a wave disturbance with wave number k, these two eigenvalues correspond to the growth rates of this wave disturbance on these two interfaces, respectively. According to the principle of most dominant eigenvalue, σ_+ corresponds to the growth rate of the more unstable (or less stable) interface for wave disturbance k since $\sigma_+(k)>\sigma_-(k)$ in general (except when $k=k_{\rm cr}$ or $k=k_*$ which exists only for some of parameter values as we have described above) and σ_- corresponds to the growth rate of the less unstable (or more stable) interface. Values of k_1 and k_2 at which two eigenvalues are zero, re-

spectively (see Fig. 2), are the widths of unstable bands for two interfaces. Since these are independent of length of the middle layer, we can recover these values of k_1 and k_2 and hence bandwidth of unstable waves [see Eq. (14)] by finding these in the limit $L \to \infty$ when instability of each of these two interfaces is described by the pure ST theory. It can easily be verified. Also, in this limit, unstable bandwidths for these two interfaces are equal to k_{cr} if the middle-layer viscosity happens to be μ_{cr}.

In summary, the length of the middle layer has no effect on the width of unstable bands for two eigenvalues and these can be determined *a priori* just by finding the bandwidth of unstable waves for each of the two interfaces individually based on the pure ST instability.

Moreover, the width of the unstable band is shortest (see Fig. 3) and equal to k_{cr} when fluid in the middle-layer has viscosity $\mu = \mu_{cr}$ regardless of the length of the middle layer. This has practical relevance: if one were to design the three-layer system which is most stable overall, it will be this viscosity μ_{cr} of the middle-layer fluid that one would choose. Interestingly, one cannot control the size of the unstable band by changing L. Then, how should one select the length L?

D. Length *L* of the middle layer and eigenvalues

It follows from Eqs. (8)–(10) that eigenvalues change exponentially fast with increasing L and as $L \to \infty$, two roots (eigenvalues) of this equation reduce to individual ST growth rates of two interfaces. Thus we recover the result that is expected on physical ground. There is another asymptotic limit, namely, $L \to 0$, when the length of the middle layer approaches zero. In this limit, this three-layer problem reduces to the pure two-layer ST problem but with a twist: two interfaces effectively act as one with effective surface tension $T+S$ within the current mathematical framework. A quick calculation shows that we recover this pure ST growth rate exactly from Eqs. (8)–(10) by letting $L \to 0$ and carrying out necessary algebraic manipulation. The manipulation removes the viscosity μ of the middle layer by cancellation which it should for consistency because the middle layer does not exist in this $L \to 0$ limit. The fact that in this limit, the merged interface has surface tension higher than the individual one will be helpful in explaining the plots in the next figure.

Below, σ_{max} is the maximum growth rate of the most dangerous wave number defined as $\sigma_{max} = \max_k[\sigma_-(k), \sigma_+(k)] = \max_k[\sigma_+(k)]$ (since $\sigma_+ > \sigma_-$). Thus, it is associated with the most unstable interface of the two for the most dangerous wave. This interface could be either the leading one or the trailing one depending on the viscosity of the middle layer and the interfacial surface tension values. Figure 4 shows plots of the maximum growth rate σ_{max} versus L for three values of the middle-layer viscosity μ with other parameters fixed at values mentioned in the caption of this figure. This figure shows that when $L=0$, σ_{max} on all three plots have the same value independent of μ according to our explanation in the previous paragraph. In fact, it is the maximum growth rate based on the pure ST theory with viscosity jump $(\mu_r - \mu_l)$ and surface tension equal to $S+T$

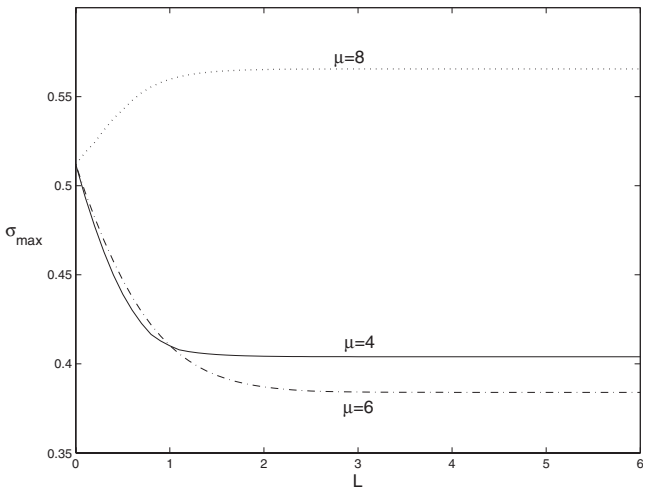

FIG. 4. Plots of σ_{max} vs L for three values of $\mu=4,6,8$ with all other parameters remaining same: $\mu_l=2$, $\mu_r=10$, $T=S=U=1$.

across the merged interface. The plot corresponding to $\mu=4$ shows the growth rate of the most dangerous wave and it is associated with the leading interface which is the most unstable among the two interfaces for the parameter values used. For these values of μ, we see that with increasing L the growth rate falls off exponentially fast to a constant positive value. Thus, the increase in L reduces the instability but does not stabilize the leading interface. The plot corresponding to $\mu=6$ is similar to $\mu=4$ but the most dangerous wave is now associated with the trailing interface instead of the leading interface. The plot corresponding to $\mu=8$ also shows the maximum growth rate of the trailing interface which is the most unstable of the two interfaces. As the length L of the middle layer increases away from *zero*, two competing effects come into play immediately for this trailing interface: instability enhancing effect of a decrease in surface tension from $(S+T)$ to S and instability suppressing effect due to a decrease in viscosity jump from $(\mu_r - \mu_l)=8$ to $(\mu - \mu_l)=6$ across this interface (see caption of Fig. 4). Overall, the result is an increase in growth rate with L of this trailing interface which settles down exponentially fast with L to the individual ST growth rate of this trailing interface. We see in the plot for $\mu=6$ the exact opposite. In summary, most of the stabilization of the leading interface for $\mu=4$ is gained exponentially fast with L and thus with small length of the middle layer. It is of the order $O(1)$ for most studies done in this context as seen in related figures. This is desirable in the context of EOR processes since it helps to keep the cost of such processes low.

E. Interfacial instability transfer mechanism

As μ exceeds μ_l, k_1 [see Eq. (4)] becomes positive and as a result long waves in the range $(0, k_1)$ on the less unstable trailing interface becomes unstable [i.e., $\sigma_- > 0 \ \forall k \in (0, k_1)$], though the same waves are more unstable on the leading interface. As the viscosity of the middle layer gradually increases toward that of the rightmost layer, the initially less unstable trailing interface (meaning all wave disturbances on the trailing interface have less growth rates than on the lead-

ing interface) eventually becomes more unstable in comparison to the leading interface (assuming both interfaces have equal surface tensions). For a disturbance of any specific wave number k, the most unstable interface which can be either the leading or the trailing one depending on the parameter values is characterized in an approximate sense by principle of dominating eigenvalue, i.e., by σ_+ since $\sigma_+ > \sigma_-$. This approximate analysis sheds light on the physics of instability transfer mechanism between the two interfaces. More importantly, it will suggest a new paradigm for interfacial instability control.

We first remark on the connection between the widths of unstable bands on two interfaces. Since k_1 as defined in Eq. (4) is a monotonically increasing function of μ and depends on surface tension S of the trailing interface, k_1 is a measure of the width of the unstable band of waves for the trailing interface as we expect it to be more and more unstable with the viscosity μ of the middle layer continuously increasing within the range $\mu_l \le \mu \le \mu_r$. However, since $\sigma_-(k_1)=0$ if and only if $\mu < \mu_{cr}$ (equivalently $k_1 < k_{cr}$) and $\sigma_+(k_1)=0$ if and only if $\mu > \mu_{cr}$ (equivalently $k_1 > k_{cr}$), the growth rate of interfacial disturbances on the trailing interface is given by σ_- when $\mu < \mu_{cr}$ and by σ_+ when $\mu > \mu_{cr}$ provided these dispersion curves for σ_- and σ_+ do not contact each other for any μ except when $\mu=\mu_{cr}$. Similarly, since k_2 is a monotonically decreasing function of μ, k_2 is a measure of the width of unstable band of waves for the leading interface as we expect increasing μ to suppress the growth of instabilities on the leading interface. However, since $\sigma_+(k_2)=0$ if and only if $\mu < \mu_{cr}$ (equivalently $k_{cr} < k_2$) and $\sigma_-(k_2)=0$ if and only if $\mu > \mu_{cr}$ (equivalently $k_{cr} > k_2$), the growth rate of interfacial disturbances on the leading interface is given by σ_+ when $\mu < \mu_{cr}$ and by σ_- when $\mu > \mu_{cr}$ provided these dispersion curves for σ_- and σ_+ do not contact each other for any μ except when $\mu=\mu_{cr}$. These instability transfer scenarios will be more involved in case the dispersion curves contact each other for some other values of μ. We do not discuss this here because for the case study we have done and discuss below, the length of the middle layer is 1 and numerical evidence suggests that for this and other parameter values used for plots in Figs. 5 and 6, the dispersion curves do not contact each other except when $\mu=\mu_{cr}$.

Figures 5 and 6 show plots of σ_- and σ_+ for values of $\mu \in [\mu_l, \mu_{cr}]$ and $\mu \in [\mu_{cr}, \mu_r]$, respectively, with $\mu_r=10$, $S=T=U=1$, and $L=1$ kept fixed. Corresponding to these values, $\mu_{cr}=6$ and $k_{cr}=2$. Figure 5 shows that the number of unstable modes for σ_- gradually increases from zero to k_{cr} and that for σ_+ decreases to k_{cr} as the viscosity μ of the middle layer gradually increases from μ_l to μ_{cr} which should enhance the instability of the trailing interface but reduce the instability of the leading interface. Therefore, for $\mu_l < \mu < \mu_{cr}$, σ_- and k_1 can be thought of as a measure of the growth rate of the less unstable trailing interface and number of unstable modes on this interface, respectively. Similarly, σ_+ and k_2 [recall that $\sigma_+(k_2)=0$], respectively, measure the growth rate of the more unstable leading interface and the number of unstable modes on this interface. Figure 6 shows that the number of unstable modes for σ_- now gradually decreases from k_{cr} and that for σ_+ increases from k_{cr} as the

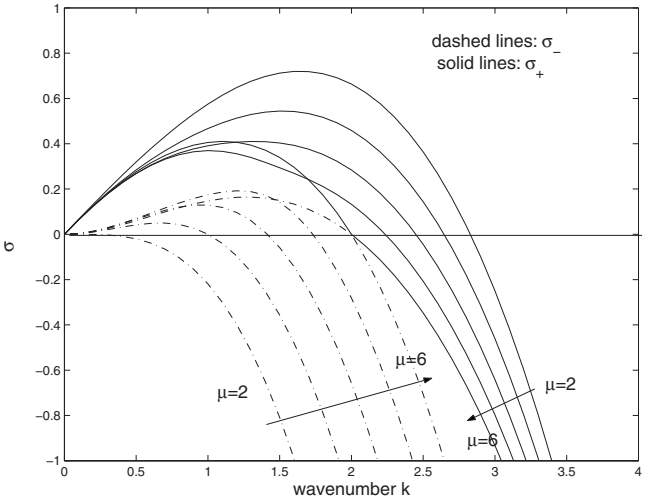

FIG. 5. Dispersion relation: growth rates σ_- and σ_+ vs wave number k for five values (2, 3, 4, 5, 6) of μ when $\mu_l=2$, $\mu_r=10$, $T=S=U=1$, $L=1$. Here $\sigma_-(k_1)=0$ and $\sigma_+(k_2)=0$ where k_1 and k_2 are defined as $k_1=\sqrt{(\mu-\mu_l)U/S}$ and $k_2=\sqrt{(\mu_r-\mu)U/T}$. For these data, $\mu_{cr}=6$, $k_{cr}=2$ [see Eqs. (12) and (13)].

viscosity μ of the middle layer gradually increases from μ_{cr}. This should make the trailing interface even more unstable and leading interface less unstable. Therefore, for $\mu > \mu_{cr}$, σ_- and k_2 $[\sigma_-(k_2)=0]$ now measure, respectively, the growth rate of the less unstable leading interface and the number of unstable modes on this interface, whereas σ_+ and k_1, respectively, now measure the growth rate of the more unstable trailing interface and the number of unstable modes on this interface. Thus, we see how the pairs (σ_-, k_1) and (σ_+, k_2) interchange their roles on the two interfaces depending on whether the middle-layer viscosity is less than or greater than the critical viscosity μ_{cr}.

We also find from plots in these figures that the most dangerous wave number k_m and corresponding growth rate $\sigma_{max}(=\sigma_{+,max})$ are decreasing functions of μ (see Fig. 5) until each of these reaches a minimum for some value $\mu=\mu_m$ and

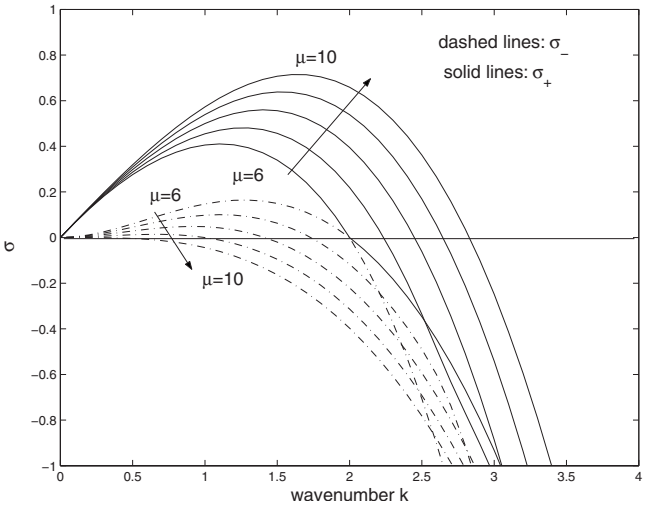

FIG. 6. Dispersion relation: growth rates σ_- and σ_+ vs wave number k for five values (6, 7, 8, 9, 10) of μ when $\mu_l=2$, $\mu_r=10$, $T=S=U=1$, $L=1$. Here $\sigma_-(k_1)=0$ and $\sigma_+(k_2)=0$ where k_1 and k_2 are defined as $k_1=\sqrt{(\mu-\mu_l)U/S}$ and $k_2=\sqrt{(\mu_r-\mu)U/T}$. For these data, $\mu_{cr}=6$, $k_{cr}=2$ [see Eqs. (12) and (13)].

thereafter for $\mu > \mu_m$, both k_m and $\sigma_{\max}$ are increasing functions of μ (see Fig. 6). In these figures, we see that μ_m is less than but close to the critical viscosity μ_{cr} ($\mu_{cr}=6$ in these figures). Thus $\sigma_{\max}(\mu)$ attains its minimum at a value $\mu = \mu_m$ which is less than μ_{cr}.

IV. UPPER BOUNDS ON THE GROWTH RATE

In Sec. V of Ref. 26 an absolute upper bound on the growth rate for the setup considered in Sec. II was briefly alluded to. Absolute and modal upper bounds in the presence of other effects were later considered in Refs. 27 and 28. In particular, an absolute upper bound in the case when the middle layer has viscosity gradient was derived in Ref. 27. By setting the viscosity gradient zero in this bound, the absolute upper bound given in Ref. 26 is recovered. In a sequel[28] to these papers, we have addressed the effect of diffusion on this upper bound. A modal upper bound derived in Ref. 28 reduces for the case of zero diffusion to the absolute upper bound given in Ref. 27.

It is important to emphasize here that the absolute upper bound alluded to in Ref. 26 and recovered from results reported in Refs. 27 and 28 as discussed above is in the form of a nonstrict inequality. This inequality there appears in a form that needs further qualification because the bound is reached in one sense (trivial case of no disturbance) but not in another sense (i.e., for a nontrivial disturbance). Since this qualification has a bearing on an attempt (see Sec. IV B) to improve upon this bound for a nontrivial disturbance, it is imperative that we first present in short a derivation of the absolute upper bound in a strict inequality form so that it is clear why that bound is not reached in practice for a disturbance. We do this next realizing that some degree of overlap of some of the material below with material published in Ref. 26 is unavoidable. Then we argue in the Sec. IV B that this upper bound can be improved if physical considerations are also taken into account. In Sec. IV B we provide such a new upper bound in this way which may be reachable in practice for some values of parameters. This new improved upper bound could not be arrived at solely based on the procedure briefly highlighted below from Refs. 26–28. Numerical evidence in support of this improved upper bound is then provided in this section.

A. A strict upper bound on the growth rate

Following the procedure mentioned in Refs. 26–28 the equation governing problem (2) is first multiplied by f, then integrated over the interval $(-L,0)$ using the boundary conditions of the problem defined in Eq. (2). This gives after simple rearrangement

$$\lambda[pf^2(0) - rf^2(-L)] = \int_{-L}^{0} f_x^2 dx + k^2 \int_{-L}^{0} f^2 dx + sf^2(-L) - qf^2(0). \tag{16}$$

From this we can write the growth rate σ as

$$\sigma = \frac{1}{\lambda} = \frac{pf^2(0) - rf^2(-L)}{\int_{-L}^{0} f_x^2 dx + k^2 \int_{-L}^{0} f^2 dx + sf^2(-L) - qf^2(0)}. \tag{17}$$

Above we have assumed f and λ to be real which is justified for the following reason. If, instead of multiplying Eq. (2) by f, we had multiplied by complex conjugate f^* of f and proceeded, then in Eq. (16) we would have $|f|^2$ instead of f^2 and $|f_x|^2$ instead of f_x^2 from which it follows that λ must be real. Since the solution f of the problem defined by Eqs. (2)–(4) for real λ is real, it then follows that f and λ are real.

Using the definitions of p, q, r, and s from Eq. (3) in Eq. (17) one finds that $\sigma > 0$ for $0 < k \leq \min(k_1, k_2)$ when both $p > 0$ and $r < 0$ [see Eq. (4)]. For these unstable modes, following inequality results from Eq. (17) after dropping two positive integrals from the denominators of Eq. (17):

$$\sigma < \frac{pf^2(0) - rf^2(-L)}{-qf^2(0) + sf^2(-L)}. \tag{18}$$

This is a strict inequality for unstable modes. All inequalities below that result from this are thus strict inequalities. From this it then follows (see Ref. 27 for details) that

$$\sigma < \max\left\{\frac{a}{c}, \frac{b}{d}\right\} = \max\left\{\left(\frac{p}{-q}\right), \left(\frac{-r}{s}\right)\right\}, \tag{19}$$

which is a modal upper bound since it depends on the wave number k. Using the definitions given in Eq. (4), the maximum values of $(p/-q)$ and $(-r/s)$ are found over range defined in inequality (15) of unstable modes and we arrive at

$$\max_k\left(\frac{p}{-q}\right) = \frac{2T}{\mu_r}\left(\frac{U(\mu_r - \mu)}{3T}\right)^{3/2}, \qquad \max_k\left(\frac{-r}{s}\right) = \frac{2S}{\mu_l}\left(\frac{U(\mu - \mu_l)}{3S}\right)^{3/2}. \tag{20}$$

Thus we obtain a strict absolute upper bound σ_u given by

$$\sigma < \sigma_u = \max\left\{\frac{2T}{\mu_r}\left(\frac{U(\mu_r - \mu)}{3T}\right)^{3/2}, \frac{2S}{\mu_l}\left(\frac{U(\mu - \mu_l)}{3S}\right)^{3/2}\right\}, \tag{21}$$

which is independent of the length L of the middle layer. Because of this strict nature of this absolute upper bound, this upper bound in practice cannot be reached. This leaves room for improving upon this upper bound. Motivated by this and inspired by physical intuition, we propose in Sec. IV B an improved absolute upper bound and validate this using numerical calculation. Before moving onto Sec. IV B, we want to re-emphasize here implications of the above result because of their importance even though some of these have been partly stressed elsewhere (see Ref. 27).

The first and the second terms in inequality (21) for the bound are NOT individual ST growth rates of two interfaces. Two functions of μ in formula (21) correspond to individual ST growth rates of two interfaces, each modified by a constant. The fact that each of these terms in Eq. (21) is different from its individual ST growth rate is due to the interfacial interactions already built into the linear model through the boundary conditions [see the problem defined in Eq. (2)].

Therefore, perhaps it is appropriate to attribute the first and second terms in Eq. (21) as strict absolute upper bounds on the "effective" growth rates of disturbances on leading and trailing interfaces, respectively. Thus, this upper bound equation (21) identifies that the growth rates of disturbances in the combined three-layer setup are smaller than the larger of the two upper bounds on effective growth rates of two interacting interfaces each of which exceeds its own individual ST growth rate.

We can recover well-known results on short wave instability in the absence of surface tensions and on two-layer flows from our results presented above for three-layer flows. For example, if the general solution to Eq. (2a) is used for $f(x)$ in Eq. (17), then one finds after simple algebraic manipulation that when $S=T=0$, $\sigma=O(k)$ for large k as expected.

The three-layer problem reduces to the pure two-layer ST problem when $S\to 0$ and $\mu=\mu_l$. From Eq. (21), an absolute upper bound denoted by σ_{su} for this case is then given by

$$\sigma < \sigma_{su} = \frac{2T}{\mu_r}\left(\frac{U(\mu_r-\mu_l)}{3T}\right)^{3/2}, \tag{22}$$

which is not less than the maximum growth rate σ_{sm} given by

$$\sigma_{sm} = \frac{2T}{\mu_l+\mu_r}\left(\frac{U(\mu_r-\mu_l)}{3T}\right)^{3/2} \tag{23}$$

for the pure two-layer ST case as it should be for consistency. Note that the case of $T\to 0$ and $\mu=\mu_r$ also gives the pure two-layer ST setup when Eqs. (22) and (23) both hold with T in these formulas replaced by surface tension S.

There is another limit, namely, $L\to 0$ (i.e., length of the middle layer approaches zero), when this problem also reduces to the pure two-layer ST problem. However, in this limit two interfaces effectively act as one with effective surface tension $T+S$. Then the maximum ST growth rate for this case is given by Eq. (23) with T in there replaced by $T+S$. Note that this is also bounded by the upper bound given above in Eq. (21). In fact, it is easy to recover this pure ST growth rate exactly from Eq. (7) by setting only $L=0$ and carrying out very easy algebraic manipulation. The manipulation removes the viscosity μ by cancellation which it should for consistency because the middle layer does not exist in this $L\to 0$ limit.

B. An improved absolute upper bound $\hat{\sigma}_u$ on the growth rate

Since the purpose of using a middle layer is to reduce the maximal ST growth rate of the interface that is pushing the most viscous fluid, the maximal ST growth rate should also be an upper bound with the following qualification: this maximal ST growth rate which we denote below by $\hat{\sigma}_{sm}$ should be based on viscosities of extreme layer fluids and the lowest interfacial surface tension coefficient of the two interfaces since the growth rate is inversely proportional to the surface tension. Thus,

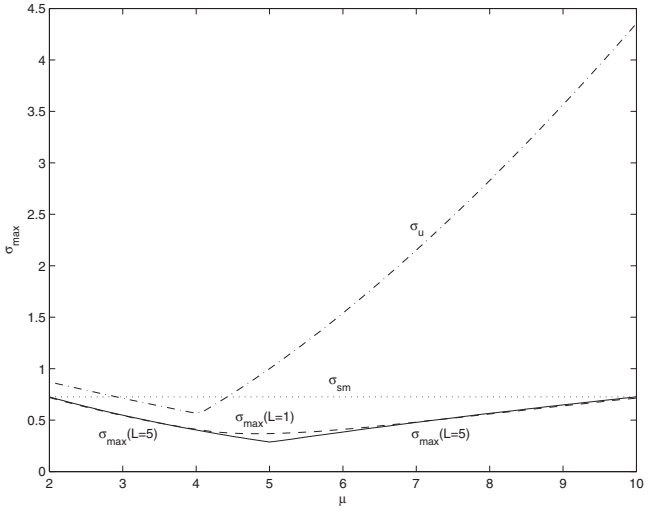

FIG. 7. Plots of the upper bound σ_u, maximal ST growth rate σ_{sm} and growth rate $\sigma_{\max}$ vs viscosity μ of the middle-layer fluid for two values (1, 5) of the length L of the middle layer with all other parameters fixed at $\mu_l=2$, $\mu_r=10$, $T=S=U=1$. The growth rate σ_{sm} is based on viscosities μ_r and μ_l. Note that for the data used here, $\sigma_{sm}=\hat{\sigma}_{sm}$.

$$\hat{\sigma}_{sm} = \frac{2\ \min(T,S)}{\mu_l+\mu_r}\left(\frac{U(\mu_r-\mu_l)}{3\ \min(T,S)}\right)^{3/2}. \tag{24}$$

There is no reason why the upper bound σ_u obtained above cannot exceed $\hat{\sigma}_{sm}$. Therefore, we conclude that an improved upper bound $\hat{\sigma}_u$ is given by

$$\sigma < \hat{\sigma}_u = \min\{\sigma_u, \hat{\sigma}_{sm}\}, \tag{25}$$

where $\mu\in(\mu_l,\mu_r)$. Note that for these values of μ, this is a strict inequality, meaning that this upper bound is not achieved in practice for $\mu_l<\mu<\mu_r$. The next plot shows merits of this new bound. Plots of $\sigma_{\max}=\max_k[\sigma_-(k),\sigma_+(k)]$, σ_u and $\hat{\sigma}_{sm}$ against μ are shown in Fig. 7 for several values of L with other parameters fixed as spelled out in the caption of the figure. These plots show that there are windows in μ where $\hat{\sigma}_{sm}$ is a better upper bound than σ_u and elsewhere σ_u is a better upper bound than $\hat{\sigma}_{sm}$. Similar plots using either μ_r or S or T as an independent variable instead of μ also show that the bound $\hat{\sigma}_u$ given by Eq. (25) is an improvement over σ_u given by Eq. (21). Such plots are not shown for the sake of conciseness. While previewing this figure, one should recall that σ_u and $\hat{\sigma}_{sm}$ do not depend on the length L of the middle layer whereas $\sigma_{\max}$ does, but it does so mildly in the sense that $\sigma_{\max}$ converges very rapidly with increasing L due to its exponential-type dependence on L. The value of μ at which the slope of the graph of $\sigma_u(\mu)$ suddenly changes can be found from Eq. (21) by equating the two functions involved in this formula.

V. CONCLUSIONS

Hydrodynamic stability of planar interfaces in a three-layer immiscible fluid flow within Hele-Shaw approximation is considered here. A fluid of constant viscosity μ_l pushes a fluid of constant viscosity $\mu>\mu_l$ which in turn pushes another fluid of constant viscosity $\mu_r>\mu$. The fluid upstream has a velocity U. The surface tension coefficients at trailing

(left) and leading (right) interfaces are taken to be S and T, respectively. We have obtained the following results based on linear theory and principle of dominant eigenvalue.

- A necessary and sufficient condition for instability of a mode with wave number k is $k < \min(\sqrt{[\mu-\mu_l]U/S}, \sqrt{[\mu_r-\mu]U/T})$. Notice that this result provides a way to control the number of unstable modes by properly adjusting one or more parameters, namely, the viscosities μ, μ_l, and μ_r and surface tension coefficients S and T. By reducing such number of unstable modes that participate initially in nonlinear evolution of interfaces, one can perhaps delay the onset of complexities in highly nonlinear regime and perhaps stabilize the flow more than otherwise possible.
- The width k_{cr} of the unstable band is shortest when $\mu=\mu_{cr}$, where μ_{cr} is given by Eq. (12) and k_{cr} is given by Eq. (13). Both of these are independent of the length L of the middle layer.
- A new upper bound $\hat{\sigma}_u$ given by Eq. (25) on the growth rate is derived. The maximum growth rate is always less than this bound [see strict inequality in Eq. (25)]. This bound in practice is never reached and hence there is a scope of further improving upon this bound. This bound is independent of the length L of the middle layer and is an improvement over earlier result. Numerical results are provided which shows that $\hat{\sigma}_u$ given by Eq. (25) is an improved upper bound over σ_u given by Eq. (21).
- Numerically and theoretically we have shown that the gain in stabilization of the leading interface is exponentially fast in the thickness of the middle layer. We have numerically explored the dependence of the extent of stabilization of the leading interface on the length of the middle layer and the viscosities of fluids in the three layers.
- When the viscosity of the middle layer is very close to the fluid it is pushing, most of the gain in stabilization of the leading interface is obtained for infinitesimally small values of L due to surface tension effect of two interfaces.
- A case study when the interfaces are close to each other is carried out to shed light on the instability transfer mechanism for this particular case. This needs a thorough and careful study in various parameter spaces due to the nature of complexity and dependence of this mechanism on various parameters of the problem. This is a topic of future study.

ACKNOWLEDGMENTS

The author is grateful to two reviewers for their constructive criticisms which have helped us improve the paper tremendously.

[1] C. M. Merle, *Multiphase Flow in Porous Media* (Editions Technip, Paris, 1981), p. 257.
[2] P. G. Saffman and G. I. Taylor, "The penetration of a fluid in a porous medium or Hele-Shaw cell containing a more viscous liquid," Proc. R. Soc. London, Ser. A **245**, 312 (1958).
[3] P. G. Saffman, "Viscous fingering in Hele-Shaw cells," J. Fluid Mech. **173**, 73 (1986).
[4] G. M. Homsy, "Viscous fingering in porous media," Annu. Rev. Fluid Mech. **19**, 271 (1987).
[5] R. L. Chouke, P. van Meurs, and C. van der Poel, "The instability of slow, immiscible, viscous liquid-liquid displacements in permeable media," Trans. Am. Inst. Min., Metall. Pet. Eng. **216**, 188 (1959).
[6] *Improved Oil Recovery By Surfactant and Polymer Flooding*, edited by D. O. Shah and R. S. Schechter (Academic, New York, 1977).
[7] R. B. Needham and P. H. Doe, "Polymer flooding review," JPT **39**, 1503 (1987).
[8] W. Littman, *Polymer Flooding: Developments in Petroleum Science* (Elsevier, Amsterdam, 1988), Vol. 24.
[9] K. S. Sorbie, *Polymer-Improved Oil Recovery* (CRC, Boca Raton, FL, 1991).
[10] Z. Zhijun and H. Yongmei, "Economic evaluation shows polymer flooding effectiveness," Oil Gas J. **100**, 56 (2002).
[11] S. B. Gorell and G. M. Homsy, "A theory of the optimal policy of oil recovery by the secondary displacement process," SIAM J. Appl. Math. **43**, 79 (1983).
[12] P. Daripa, J. Glimm, B. Lindquist, and O. McBryan, "Polymer floods: A case study of nonlinear wave analysis and instability control in tertiary oil recovery," SIAM J. Appl. Math. **48**, 353 (1988).
[13] S. Grossmann, "The onset of shear flow turbulence," Rev. Mod. Phys. **72**, 603 (2000).
[14] M. Nishioka, S. Iida, and Y. Ichikawa, "An experimental investigation of the stability of plane Poiseuille flow," J. Fluid Mech. **72**, 731 (1975).
[15] P. G. Drazin and W. H. Reid, *Hydrodynamic Stability* (Cambridge University Press, London, 1981), p. 527.
[16] P. Daripa and G. Pasa, "An optimal viscosity profile in enhanced oil recovery by polymer flooding," Int. J. Eng. Sci. **42**, 2029 (2004).
[17] P. Daripa and G. Pasa, "New bounds for stabilizing Hele-Shaw flows," Appl. Math. Lett. **18**, 1293 (2005).
[18] G. Bayada and M. Chambat, "The transition between the Stokes equations and the Reynolds equation—A mathematical proof," Appl. Math. Optim. **14**, 73 (1986).
[19] S. A. Nazarov, "Asymptotic solution of the Navier–Stokes problem on the flow of a thin layer fluid," Sib. Math. J. **31**, 296 (1990).
[20] E. Sanchez-Palencia, *Non-Homogeneous Media and Vibration Theory* (Springer-Verlag, Berlin, 1980), p. 398.
[21] J. Bear, *Dynamics of Fluids in Porous Media* (Dover, New York, 1974), p. 764.
[22] Z. Yang and Y. C. Yortsos, "Asymptotic solutions of miscible displacements in geometries of large aspect ratio," Phys. Fluids **9**, 286 (1997).
[23] M. Shariati, L. Talon, J. Martin, N. Rakotomalala, D. Salin, and Y. C. Yortsos, "Physical origins of the change of type from hyperbolic to elliptic equations: Fluid displacement between two parallel plates," J. Fluid Mech. **519**, 105 (2004).
[24] F. J. Hickernell and Y. C. Yortsos, "Linear stability of miscible displacement processes in porous media in the absence of dispersion," Stud. Appl. Math. **74**, 93 (1986).
[25] A. De Wit, Y. Bertho, and M. Martin, "Viscous fingering of miscible slices," Phys. Fluids **17**, 054114 (2005).
[26] P. Daripa and G. Pasa, "On the growth rate for three-layer Hele-Shaw flows: Variable and constant viscosity cases," Int. J. Eng. Sci. **43**, 877 (2005).
[27] P. Daripa and G. Pasa, "A simple derivation of an upper bound in the presence of viscosity gradient in three-layer Hele-Shaw flows," J. Stat. Mech.: Theory Exp., No. P01014, January 2006.
[28] P. Daripa and G. Pasa, "Stabilizing effect of diffusion in enhanced oil recovery and three-layer Hele-Shaw flows with viscosity gradient," Transp. Porous Media **70**, 11 (2007).